Toward Improved Bioremediation Strategies: Response of BAM-Degradation Activity to Concentration and Flow Changes in an Inoculated Bench-Scale Sediment Tank

Fengchao Sun, Adrian Mellage, Zhe Wang, Rani Bakkour, Christian Griebler, Martin Thullner, Olaf A. Cirpka, and Martin Elsner*

Read Online

ACCESS | Metrics & More | Article Recommendations | Supporting Information

ABSTRACT: Compound-specific isotope analysis (CSIA) can reveal mass-transfer limitations during biodegradation of organic pollutants by enabling the detection of masked isotope fractionation. Here, we applied CSIA to monitor the adaptive response of bacterial degradation in inoculated sediment to low contaminant concentrations over time. We characterized *Aminobacter* sp. MSH1 activity in a flow-through sediment tank in response to a transient supply of elevated 2,6-dichlorobenzamide (BAM) concentrations as a priming strategy and took advantage of an inadvertent intermittence to investigate the effect of short-term flow fluctuations. Priming and flow fluctuations yielded improved biodegradation performance and increased biodegradation capacity, as evaluated from bacterial activity and residual concentration time series. However, changes in isotope ratios in space and over time evidenced that mass transfer became increasingly limiting for degradation of BAM at low concentrations under such stimulated conditions, and that activity decreased further due to bacterial adaptation at low BAM (μg/L) levels. Isotope ratios, in conjunction with residual substrate concentrations, therefore helped identifying underlying limitations of biodegradation in such a stimulated system, offering important insight for future optimization of remediation schemes.

KEYWORDS: *2,6-dichlorobenzamide (BAM), bioavailability, compound-specific isotope analysis (CSIA), mass-transfer, priming effect*
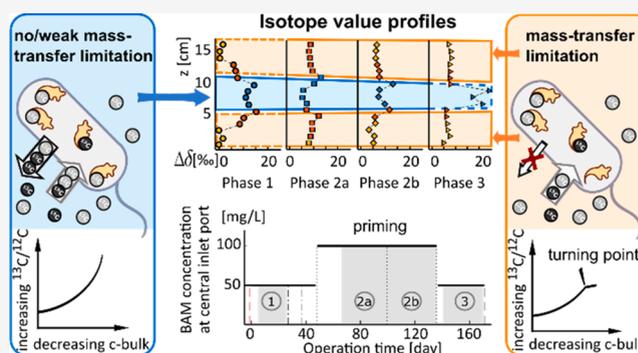
INTRODUCTION

Anthropogenic groundwater pollution by organic chemicals has become a serious concern for potable water supply, human health, and natural ecosystems.[1−3] Although many organic pollutants are biodegradable, they are frequently detected in the environment and wastewater treatment plants at microgram- to nanogram-per-liter concentrations, even under nutrient- and biomass-rich conditions (e.g., field sites or specially designed bioaugmented sand filters). Understanding the limitations of organic micropollutants biodegradation, or their persistent metabolites, and improving bioremediation strategies and approaches are, therefore, prominent current research challenges.[1]

BAM (2,6-dichlorobenzamide), a metabolite of the widely applied herbicide dichlobenil and of the fungicide fluopicolide, is a typical example of a mobile organic micropollutant. It has been frequently detected above drinking water thresholds (0.1 μg/L)[4] in groundwater in many European countries[5−8] and may affect human (slightly toxic by oral route)[9] and ecosystem health (i.e., moderate ecotoxicity to freshwater species).[10] With a high water solubility of 2.7 g/L, a low log K_{ow} of 0.77, and a low K_d of 0.10−0.93 L/kg, it is extremely mobile in groundwater and adsorption to aquifer sediments is negligible.[11] To purify BAM-polluted groundwater, bioremediation is an effective approach both in situ and ex situ by deploying sand filters augmented with BAM-degrading bacteria.[5,12−18] The so far best-studied strain for BAM biodegradation is *Aminobacter* sp. MSH1, an aerobic, Gram-negative, motile but potentially nonchemotactic[19] strain that can completely mineralize BAM as sole source of carbon, nitrogen, and energy[5] without accumulation of intermediates.[15] The complete catabolic degradation pathway has recently been elucidated in detail.[20] The conversion of BAM to 2,6-dichlorobenzoic acid (2,6-DCBA) is considered the key step

of the overall process,[21] whereas further transformation of 2,6-DCBA is comparatively rapid in sand filters.[6]

However, a specific challenge of using *Aminobacter* sp. MSH1 for BAM degradation is that the rate of BAM degradation appears to decrease over time in long-term purification schemes.[5,15,22] A manifestation of this phenomenon is the observation that the degree of biodegradation, that is, the extent to which concentrations decrease relative to their initial value for a given residence time, drops at low BAM concentrations.[5,22,23] One explanation of this decreased degree of BAM biodegradation is the loss of inoculated bacteria from sediments, irrespective of whether the sand filters were running with or without backwashing.[5,15] Due to the loss of inoculated bacteria (e.g., via protozoan grazing,[5,16] competition with indigenous bacteria,[5] and wash-out[15]), BAM degradation efficiency can decrease to less than 20% from the initial degradation/mineralization rate, and it has been reported to be difficult to maintain efficient degradation for more than 2 to 3 weeks.[15,22] A second possible explanation for poor long-term performance of biofilters is starvation of degraders. In the study of Horemans et al.,[18] even though the degrading biomass in the sand filters should not limit BAM degradation based on theoretical considerations, specific BAM degradation rates were 100-fold below expectations. This is consistent with observations of Sekhar et al.[5,23] where 30−60 day-old cells in carbon- and nitrogen-starved biofilms grew slower compared to fresh cells, likely because of reduced bacterial fitness (physiological adaptation).[23] In general, observed degradation efficiency at low BAM concentrations was consistently smaller compared to biodegradation at high BAM concentrations.[8] Studies have argued that a potential limiting factor for biodegradation of BAM at low concentrations, that is, under starvation/oligotrophic conditions, is rate-limiting mass transfer of the contaminant from the bulk solution into the bacterial cell.[24,25] In addition, physiological limitations that decrease the overall enzymatic activities inside bacterial cells may be a factor, such as detachment or death of cells, down-regulation of functional genes, or reduced activity of catabolic enzymes due to a physiological response to oligotrophic conditions.[23,26]

Perturbations via transient contaminant supply or flow fluctuation in flow-through sediment systems have shown promise in enhancing and recovering the efficiency of bacterially mediated contaminant biodegradation.[14,27] Evidence has shown that transient flow and/or transient contaminant loads may spread microbial biomass over a larger area and maintain gene expression at a sufficient level, yielding an improved degradation capacity.[27−31] In addition, in most natural microbial environments, microbes will show characteristic switches between growth-supporting state (high-nutrient flux *r* condition) and maintenance state (low-nutrient flux *K* condition) in response to the related environmental stress for microbial fitness, such as a temporary change in food supply or population density.[32] Many studies suggest that bacteria preadapted to a given target contaminant at a certain threshold concentration may stay active even at low contaminant concentrations or regain biodegradation ability faster than bacteria that have not been exposed to the contaminant before.[14,27,33−36] However, knowledge gaps still remain regarding (i) to what extent bacterial adaptation happens in response to different system perturbations, (ii) whether bacterial adaptation under system perturbations can yield promising degradation efficiency over a long time, and (iii) how to recognize the underlying limitations (physiological vs

mass-transfer limitation) in response to such system perturbations.

To address these knowledge gaps, we applied compound-specific stable isotope analysis (CSIA), an advanced approach for the interpretation of biodegradation. The isotope value of a substrate/organic contaminant in a sample is usually expressed as δ [‰],

$$\delta_{\text{sample}} = \frac{R_{\text{sample}} - R_{\text{standard}}}{R_{\text{standard}}} \quad (1)$$

in which the heavy to light isotope ratio (e.g., $^{13}C/^{12}C$, $^{15}N/^{14}N$) of a sample R_{sample} [−] is reported relative to the isotope ratio of an international reference material R_{standard} [−]. For example, Vienna PeeDee Belemnite (V-PDB) and Air-N_2 are the international reference standards for carbon and nitrogen isotope values, respectively. As recently demonstrated by Sun et al.[37] and other laboratory[38] and field studies,[39] isotope fractionation induced by dispersion, diffusion, and adsorption in aqueous phase and porous media is negligible, whereas enzymatic biotransformation causes pronounced changes in isotope values of BAM.[40] Observation of such pronounced isotope fractionation may therefore be linked to degradation, and the absence of isotope fractionation despite ongoing BAM degradation may uniquely inform about rate-limiting mass transfer into the cell interior.

Specifically, since the enzymatic reaction of the first step in BAM transformation is associated with a pronounced isotope effect,[40] BAM molecules with heavy isotopes are discriminated during enzyme turnover. When this intracellular enzyme turnover is slower than mass transfer into and out of the bacterial cell, molecules can diffuse freely in and out making this isotope fractionation observable in the bulk solution that is sampled for analysis.[24] Such pronounced isotope fractionation during biotransformation is usually observed at high substrate concentrations, and is described by the Rayleigh equation, which has been widely applied for well-mixed closed systems (eq 2, Figure 1c, left).[41,42] It is applicable if a unidirectional enzymatic reaction is rate limiting such that the ratio of pseudo first-order rate coefficients of two isotopologues is constant.[43,44]

$$\frac{(^{h}c/^{1}c)_t}{(^{h}c/^{1}c)_0} = \frac{\delta_t + 1}{\delta_0 + 1} = f^{\varepsilon} \quad (2)$$

In eq 2, ^{h}c [μg/L] and ^{1}c [μg/L] represent the concentration of heavy and light isotopologues, respectively; $f = c_t/c_0$ [−] represents the remaining fraction of the substrate; δ_0 [‰], and δ_t [‰] represent the isotope values at time zero and at time t, respectively; ε [‰] is the ratio of the pseudo first-order rate coefficients, the isotope enrichment factor.

By contrast, when enzyme turnover is faster than diffusive substrate supply into (and out of) the cell, mass transfer becomes rate-limiting.[24] Hence, substrate molecules are consumed in enzyme turnover before they can diffuse back to the outside of the cell. Consequently, changes in substrate isotope ratios of the cell interior are no longer reflected in the bulk solution: observable isotope fractionation is masked (Figure 1c, right).[24,45,46] A decrease in isotope fractionation beyond the trend expected from Rayleigh fractionation is, therefore, indicative of mass-transfer limitations. Such a transition has been observed specifically at low concentrations in various experimental setups with either suspended cells or
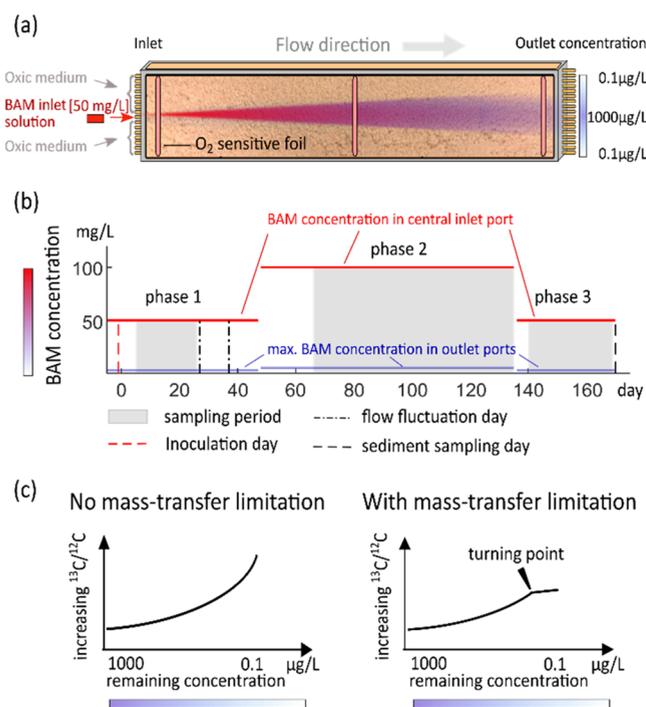
Figure 1. (a) Simplified tank setup and the sketch of the plume shape. (b) Sequence of experimental phases with BAM inlet concentration of 50 mg/L (phase 1), 100 mg/L (phase 2), and 50 mg/L (phase 3) at the central inlet port ($z = 8$ cm) yielding μg/L concentrations at the outlet ports. Gray shades: periods over which integrated samples were taken for isotope analysis at quasi-steady state; red dashed line: day of inoculation; dash-dotted lines: days of flow fluctuation; dashed line: day of sediment sampling for attached bacterial cell number counting (day 170). (c) Conceptual sketches of expected isotope fractionation with decreasing concentrations without (left) and with (right) mass-transfer limitation.

attached cells on sediments adapted to oligotrophic concentrations.[45−48]

Whether or not this effect will be observed when bacteria adapt to low concentrations, however, is an open question. Evidence has shown that bacteria can downregulate their overall enzyme activity in response to surrounding low concentrations, slowing down enzymatic turnover to match slow mass transfer (physiological adaptation).[26] In this case mass transfer may not necessarily be limiting and isotope fractionation following the Rayleigh equation might also be observed at low concentrations (Figure 1c, left). Furthermore, mass-transfer limitation and downregulation of enzymatic turnover might not be mutually exclusive, but rather go hand in hand. By using isotope fractionation as a performance indicator, we can, therefore, characterize changes in biodegradation activity and enzyme regulation in response to perturbations and identify the underlying limitations when a system is operating under different quasi-steady-state conditions.

In this study, we therefore characterized the response and adaptation of microbial BAM degradation in a flow-through sediment tank inoculated with the BAM-degrading bacterial strain *Aminobacter* sp. MSH1, exposed to a transient supply of elevated contaminant concentrations as a priming strategy (Figure 1). In addition, we took advantage of an inadvertent temporal flow fluctuation in the sediment system to investigate how the perturbations changed bacterial activity and the

associated biodegradation efficiency in space and over time. By injecting an anoxic BAM solution through a single, central inlet port of the tank while injecting a BAM-free oxygen-saturated solution through parallel ports above and below, we created transverse cross-gradients of BAM and dissolved oxygen. Thus, concentrations (μg/L) at the fringes of the BAM plume (near the upper and lower boundaries of the tank, Figure 1) mimicked typical oligotrophic conditions in groundwater or raw water-treatment facilities (e.g., sand filters). The vertical distribution of concentrations, biomass, and isotope fractionation along the outlet of the tank enabled us to track changes in bacterial adaptation and biodegradation activity at different concentrations, and to identify the concentration range at which mass transfer and physiological adaptation were, or became, limiting. In addition, the upper and lower regions of the tank can be regarded as physical/technical replicates because they were operated under identical external conditions (i.e., homogeneous sediment conditions with identical flow rates). We increased the inlet substrate concentration as a priming strategy to stimulate biomass growth and the degradation activity of the bacterial strain. Subsequently, we decreased the inlet concentration back to the initial conditions. In a recent study, we modeled a subset of this experimental data corresponding to a momentary steady-state profile as a proof-of-principle to reveal the relevance of mass transfer through the cell membrane as a limiting factor for biodegradation at low contaminant concentrations.[46] The present study takes one step further to investigate the relevance of mass-transfer limitation not only during a single snapshot in time, but continuously throughout the adaptation of an inoculated system. Thus, it places the newly discovered and confirmed isotope approach into practice by analyzing the long-term adaptation of the system (e.g., enzyme activity, mass-transfer limitation) and its response to concentration and flow changes. Here, isotope analysis served to explore the factors (namely mass transfer or bacterial physiology) that represented different bottlenecks of degradation while actively engineering the system toward improved bioremediation of the organic micropollutant BAM.

■ EXPERIMENTAL SECTION

Setup of the Quasi-Two-Dimensional Flow-Through Sediment-Tank. The setup of the tank system was adapted from Bauer et al.[49] and has been detailed in Sun et al.[37,46] Briefly, the tank with inner dimensions of 95 cm × 18 cm × 1 cm (Figure 1a, quasi-two-dimensional) was wet-packed with uniform quartz sand (diameter of 0.8−1.2 mm). Sixteen equally spaced (1.0 cm) ports were emplaced at the inlet and outlet of the tank. An anoxic BAM solution was injected at the center of the inlet ports (at $z = 8$ cm), whereas oxic medium was introduced through the other inlet ports, and samples were collected at quasi-steady state at the outlet ports. This gave rise to low (microgram-per-liter) concentrations in the vertical gradient at the outlet ports of the tank. During all the experimental stages (e.g., abiotic experiment, inoculation, and biotic experiments), the pumping rate of all ports was maintained at 45 ± 2 μL/min/port (with a seepage velocity of 1.25 m/day, and residence time of 18.2 h). Detailed information about the preparation and setup of the tank experiment, chemicals, liquid media, and bacterial cultures is provided in the Supporting Information (SI).

Before the inoculation, the tank was operated in an abiotic experimental phase to establish a stable, conservative

concentration distribution in the tank by continuously injecting a 50 mg/L sterilized, anoxic BAM solution at the central inlet port (at z = 8 cm) and a sterilized oxic medium through all other inlet ports (SI Figure S3). As observed in other studies[27,49,50] with a similar setup and a homogeneous porous medium, the conservative tracer behavior in the tank system[51] showed a symmetrical concentration distribution along the vertical outlet profile of the tank. After running the abiotic experiment for 4 days, a stable, conservative plume established.[37] Subsequently, we started the biotic experiment by introducing an inoculum (without carbon or nitrogen source) of the strain *Aminobacter* sp. MSH1 (with a cell density of 1×10^7 cells/mL) to all ports except the central one for 24 h. After inoculation, we stopped the flow for 3 h to allow the bacteria to adhere to the sediment. The first day after the inoculation was denoted day 1. The experiment consisted of three phases (Figure 1b), with sequential changes of the BAM inlet concentration through the central port from 50 mg/L (phase 1) to 100 mg/L (phase 2), and back to 50 mg/L again (phase 3). Specifically, in phase 1, we injected a 50 mg/L BAM solution through the central port, and all concentrations in the respective outlet ports were at quasi-steady state from day 5 to day 26. On day 27 and day 35, flow inadvertently fluctuated due to partial blockage of individual tubes connected to the outlet ports such that the system was not at steady state anymore during a short intermittence. After normal flow was reestablished, we started phase 2 of the experiment by increasing the BAM inlet concentration through the central port to 100 mg/L on day 50. The concentrations in the outlet reached a quasi-steady state on day 66. The system continued running at 100 mg/L BAM inlet concentration until day 135. On day 136, we decreased the inlet BAM concentration through the central port back to 50 mg/L (phase 3). During the last experimental period from day 140 to day 169, changes of concentrations were minimal, yielding a quasi-steady state. At the end of the experiment (day 170), sediment samples were collected from the tank in different depths along different vertical cross sections.

Samples for concentration measurements of BAM and its metabolite 2,6-dichlorobenzoic acid (2,6-DCBA), isotope measurements, and bacterial cell counting (TCC_{out}) were collected at each outlet port. In each experimental phase, concentration samples (1 mL) were taken every 3 to 5 days, while samples for isotope analysis were continuously collected until one to two liters of sample for isotope analysis had accumulated at each outlet position. In phase 1, with 50 mg/L BAM inlet concentration at the central port, samples for isotope analysis were collected from day 5 to day 26. In phase 2, with a 100 mg/L BAM inlet concentration at the central port, we collected isotope samples over two periods, from day 66 to day 98 and from day 99 to day 135. The quasi-steady-state data from the second sampling period (phase 2) has been presented by Sun et al.[46] as a subset of the results discussed in full here. In phase 3, with the BAM inlet concentration at the central port back to 50 mg/L, we collected isotope samples from day 140 to day 169 (Note: All sampling times are given in days after inoculation). Samples for concentration and isotope measurements were all filtered through 0.22 μM syringe filters (Merck KGaA, Germany) and stored at -20 °C until analysis.

Stable Carbon Isotope Analysis of BAM. Biodegradation of BAM by *Aminobacter* sp. MSH1 has previously been shown to induce strong carbon isotope fractionation with isotopic enrichment factors ε_C = $-7.8 \pm 0.2‰$ at high

concentrations in batch experiments.[40] For the carbon isotope measurements of BAM, samples concentrated in ethyl acetate after solid-phase extraction (SPE) were measured on a GC-IRMS system in which a TRACE GC Ultra gas chromatograph (Thermo Fisher Scientific, Italy) was coupled to a Finnigan MAT 253 isotope-ratio mass spectrometer (IRMS) through a Finnigan GC Combustion III interface (Thermo Fisher Scientific, Germany). The separation was carried out on a DB-5 analytical column (60 m, 0.25 mm i.d., 0.5 μm film, Agilent Technologies, Germany). The typical uncertainty of carbon isotope measurements is $\pm0.5‰$. A detailed method description, including sample preparation and SPE, is provided in the SI.

Concentration Measurements of BAM, DO, and Total Cell Counts. By adopting the method of Jensen et al.,[52] concentrations of BAM and 2,6-DCBA were measured by liquid chromatography-tandem mass spectrometry (LC-MS/MS) after SPE for sample preparation. Compound separation was performed using a Kinetex C18 column (2.6 μm, 10 nm, 100 $\times$ 2.1 mm i.d., Phenomenex, U.S.) at 40 °C. A detailed method description is provided in the SI. We calculated the fraction f [$-$] of residual BAM concentrations c_{BAM}^{biotic} [μg/L] relative to the initial BAM concentrations $c_{BAM}^{abiotic}$ [μg/L] that would be expected in the absence of biodegradation,

$$f = c_{BAM}^{biotic} / c_{BAM}^{abiotic} \tag{3}$$

Here, $c_{BAM}^{abiotic}$ values for 50 mg/L BAM concentrations at the central inlet port were inferred from the concentration profile on the fourth day of the initial abiotic experiment (see above and Sun et al.[37]). $c_{BAM}^{abiotic}$ values for 100 mg/L inlet concentrations at the center port were extrapolated from the $c_{BAM}^{abiotic}$ values of the 50 mg/L inlet concentration condition considering that transverse dispersion scales linearly with concentrations so that values in the profile can be multiplied by an appropriate factor (here: 2).

DO concentrations along the vertical cross sections at the inlet, in the middle, and at the outlet of the tank were monitored by reading oxygen-sensitive polymer optode foils (18 cm $\times$ 0.5 cm, PreSens GmbH, Regensburgs, Germany) at the inner side of the tank with a FIBOX2 Fiber-optic oxygen meter (PreSens, Regensburg, Germany). For total cell counts of the washed-out bacteria, samples (1.5 mL) were collected every 3−5 days from the outlet ports of the tank, fixed with glutaraldehyde (2.5% final concentration), and stored at 4 °C. For the total cell counts of the attached bacteria on the sediments, duplicate sediment samples (0.5 mL) were taken at every 1.0 cm depth (from z = 1 cm to z = 16 cm) along the vertical cross sections at 2 cm distance from the inlet boundary, in the middle, and at 2 cm from the outlet boundary of the tank at the end of the experiment on day 170. A detailed description of sediment sampling and sample treatment is provided in the SI. Samples for the bacterial cell number measurement were stained with SYBR Green I and measured on a Cytomics FC 500 flow cytometer (Beckmann Coulter, Hebron, KY) according to the method of Bayer et al.[53] To further confirm the presence of the strain *Aminobacter* sp. MSH1 and to probe for potential contamination (which would not be seen by qPCR) at all depths (z) of the tank, terminal restriction fragment length polymorphism (T-RFLP) analysis was performed to target bacterial 16S rRNA genes. DNA isolation was done for samples collected at each depth at the end of the experiment according to the protocol described
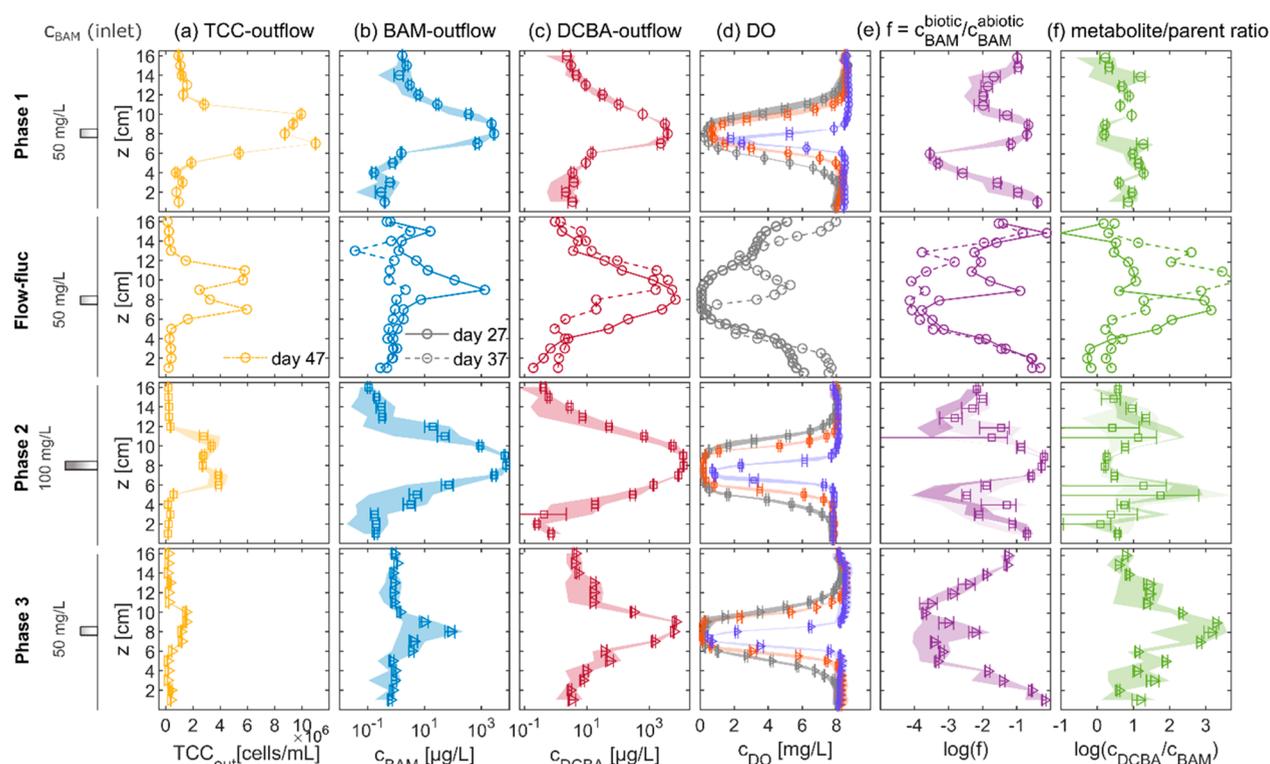
Figure 2. Vertical profiles of washed-out cell numbers, concentrations, and concentration ratios. Column (a): total number of washed-out cells; column (b): BAM concentrations; column (c): 2,6-DCBA concentrations; column (d): dissolved oxygen (DO) concentrations 2 cm from the inlet boundary (blue shade), in the middle of the tank (orange shade), and 2 cm from the outlet boundary (gray shade); column (e): residual BAM concentrations in the effluent relative to the expected concentration in an abiotic experiment $f = c_{BAM}^{biotic}/c_{BAM}^{abiotic}$, see eq 3; column (f): molar concentration ratios of 2,6-DCBA to BAM in the effluent in three experimental phases and on the flow fluctuation days. Color shades represent the range of measurement values during the sampling periods. Data points with error bars represent the average values with standard errors during the quasi-steady state sampling periods. DO profiles on the flow fluctuation days only represent the data measured along the outlet cross-section. Samples for concentration measurements were measured every 3 to 5 days from days 5 to 26, 66 to 135, and 140 to 169. Samples for TCC_{out} measurements were measured on days 17, 19, 47 (phase 1), 81, 83, 87 (phase 2), 155, and 159 (phase 3), respectively.

in Pilloni et al.[54] The PCR thermo profile (SI Figure S5) and T-RFLP process are further described in the SI.

■ RESULTS AND DISCUSSION

Distribution of Solutes and Biomass. Figure 2 summarizes results of the three experimental phases with BAM inlet concentrations in the central port of 50 mg/L, 100 mg/L, and 50 mg/L, respectively, as well as snapshots during the phase of flow-fluctuation at the end of phase 1. The vertical profiles in the three phases show the typical plume-fringe pattern,[14,27,49] that is, the hot spots of biomass growth (reflected in the washed-out cell number) were located at the plume fringes where BAM and DO mixed due to transverse dispersion, and steep DO concentration gradients developed toward the plume center. At the hot spots in the plume fringes, BAM degradation was most efficient, indicated by the lowest fraction *f* and the highest ratio of 2,6- DCBA to BAM concentrations (Figure 2e,f). In the plume center, the washed-out cell numbers (a proxy for growth) were lower than at the plume fringes, and the remaining BAM and 2,6-DCBA concentrations were highest indicating that the lack of electron acceptor (i.e., DO) limited biodegradation of BAM and biomass growth. In the uppermost and lowermost regions of the tank, low μg/L-level concentrations and low biomass densities adequately mimicked oligotrophic conditions typical of groundwater or sand-filter systems. Even though at these locations the electron acceptor (i.e., DO) was in excess,

degradation efficiency was lower than at the plume fringes, with a higher *f*-value and a lower molar concentration ratio of 2,6-DCBA to BAM. The observed decrease in BAM degradation capacity with decreasing BAM concentrations (from the plume fringes to the uppermost and lowermost regions of the plume, Figure 2f) were consistent with the reduced BAM degradation activity of *Aminobacter* sp. MSH1 at low concentrations observed in batch and flow channel studies.[8,23,55] The lower bacterial degradation activity at low concentrations will be discussed together with the results from isotope analysis below.

To better understand bacterial adaptation in the different zones of the BAM plume, we calculated the ratio of the number of sediment-attached bacteria to the washed-out bacterial cell number per unit of bulk volume (TCC_{sed}/TCC_{out}) at the end of phase 3 with 50 mg/L BAM inlet concentration (Figure 3). When calculating the ratio TCC_{sed}/TCC_{out}, the number of washed-out (suspended) bacterial cells per unit of water volume (cells L_{liquid}^{-1}) was transformed into the number of bacterial cells per unit of bulk volume (cells L_{bulk}^{-1} = cells L_{sed}^{-1}) by multiplication with the porosity of 0.45. The number of bacteria attached to the sediment was 13−220 times higher than the number of washed-out bacterial cells. In the center of the plume ($z = 7−10$ cm), where there was no substrate (BAM) limitation, the ratio of attached to suspended cells (TCC_{sed}/TCC_{out}) was the smallest. With the widening of the plume, this ratio increased. This trend of the
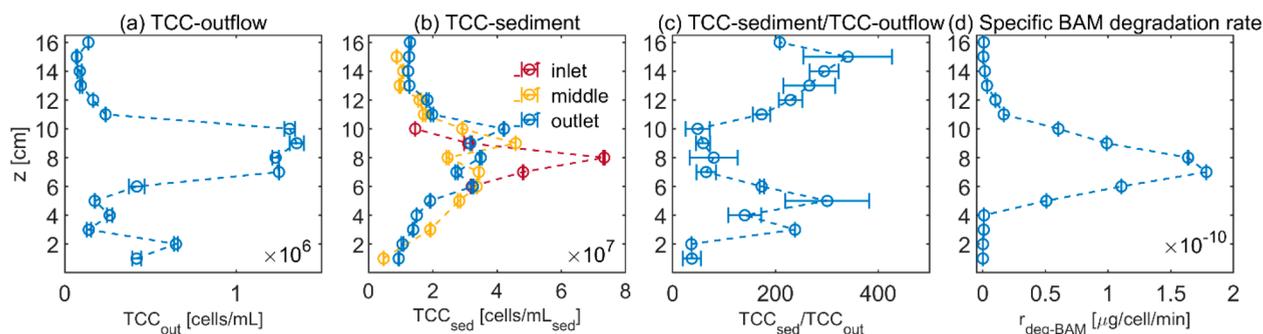
Figure 3. Vertical profiles of (a) total cell number of washed-out bacteria (TCC_{out}), (b) total cell number of bacteria attached to the sediments (TCC_{sed}) on the last sampling day of phase 3 (day 170) with 50 mg/L inlet concentration, (c) ratio of the cell number on sediments to the washed-out cell number per unit of bulk volume, (d) specific BAM degradation rate per cell $r_{deg-BAM}$ on day 170. In panel (b), red, yellow, and blue circles represent the measurements of TCC_{sed} at 2 cm distance from the inlet boundary, in the middle, and at 2 cm distance from the outlet boundary of the tank, respectively. Error bars in panel (a)−(b) represent the measurement errors (standard deviation); uncertainties in panel (c)−(d) were calculated based on Gauss' error propagation law by using the standard deviations of TCC_{sed} values at different locations.

TCC_{sed}/TCC_{out} ratio (Figure 3c) mirrors the observations in many microcosm[28,56] and field studies[57−61] in which a low TCC_{sed}/TCC_{out} ratio occurs at high substrate concentrations, whereas a high TCC_{sed}/TCC_{out} ratio, albeit with overall lower absolute cell numbers, is typical of substrate-limited oligotrophic conditions.[57,62] This pattern has been explained by the growth/cell-division-mediated biomass transport in previous studies:[28,33,63] when a certain density of the attached biomass in microcolonies is reached (carrying capacity), additional bacteria cells resulting from biomass growth (i.e., cell division) are released into the mobile phase and can thus be washed out.[63] Column experiments conducted by Mellage et al. suggest that the release of daughter cells during growth is orders of magnitude higher than cell detachment driven by alternative mechanisms, and as such these can be neglected.[33] Therefore, the increased TCC_{sed}/TCC_{out} ratio, observed in our experiment, at smaller substrate concentrations indicates slower microbial growth at lower concentrations. We therefore divided the BAM-mass consumed per time by the cell number of the attached bacteria to obtain the specific BAM-degradation rate per cell $r_{deg-BAM}$. In general, we observed a decreased $r_{deg-BAM}$ with decreasing BAM concentration, which indicated that the observed trend in the fraction f of transformed BAM in phase 3 (Figure 2e, fourth row) was not only due to a lower number of attached bacteria at low concentrations (Figure 3b), but also to a lower cell-specific degradation activity (Figure 3d).

Adaptation of *Aminobacter* sp. MSH1 and Biodegradation Efficiency. In phase 1 of the experiment, when we introduced 50 mg/L BAM through the central port, biodegradation of BAM started immediately after inoculation, and the system remained at quasi-steady state from day 5 to day 26. The relatively high number of washed-out cells (Figure 2a, first row) indicated that bacteria may have been in an adaptation stage after inoculation, where they showed a lower tendency to attach to sediment. In addition, a fraction of these washed-out cells may stem from the original inoculation. Interestingly, the spatial distribution of the biodegradation activity was not yet symmetric, with a smaller f-value at the lower than at the upper fringe of the plume (Figure 2e, first row). This observed asymmetrical distribution of f-values indicates that the inoculation-induced activity of bacteria was still different in the two replicate parts of the tank, even after 3 weeks of operation. This may be caused by a nonsymmetric

distribution of microbial activity, possibly in combination with slight variations in flow and/or bacterial adaptation.

At the end of phase 1, inadvertent partial "clogging" occurred shortly in the outlet ports on day 27 and day 35, which provided an opportunity to investigate the response of the system to a flow fluctuation. The plume of BAM slightly shifted upward along with a concomitant fluctuation of 2,6-DCBA (Figure 2) and DO (SI Figure S2). More BAM was degraded as indicated by decreased BAM concentrations (Figure 2b, second row) and a decreased f-value (Figure 2e, second row). After the clogging was removed, the previous flow regime re-established, and the plume went back to its original position. The BAM concentrations remained at lower levels in conjunction with a smaller number of washed-out bacterial cells by the end of the first period (day 47). The low remaining BAM concentrations indicated an enhanced degradation of BAM due to a better spread of the bacterial biomass driven by flow fluctuation.[27,28,31] Specifically, when the plume center slightly shifted upward—as indicated by the shift of the conservative tracer metolachlor (Figure S1)—it reached the previous plume fringes where biomass hot spots were located. In addition, a shift of the BAM plume induced a shift in the distribution of biomass, leading to a buildup of cells at new locations (as depicted in Figure 2a second row, the hot-spot fringe shifted upward from $z = 10$ cm to $z = 11$ cm). Thus, the flow fluctuation (i.e., reduction of the flow rate and redirection of the plume due to the clogging) led to an unintended priming which stimulated a more even distribution of biodegradation activity throughout the spatial profile.

In phase 2, we increased the BAM concentration in the central inlet port to 100 mg/L, establishing a quasi-steady state after 2 weeks. Even though the increased inlet concentration would be expected to induce a higher growth rate of attached biomass, the numbers of washed-out cells were smaller than in phase 1 and during the flow fluctuation period. The smaller washed-out cell numbers in phase 2 may indicate that bacteria were not yet well adapted until phase 2. Under the assumption that washed-out cell numbers represented cell growth, we calculated the carbon assimilation rate by dividing the amount of consumed carbon of BAM and 2,6-DCBA to the amount of carbon of the washed-out biomass (SI Table S2). The calculated carbon assimilation rate of $17 \pm 10\%$ indicates that carbon was primarily utilized for cell respiration rather than cell growth (carbon assimilation for biomass synthesis).
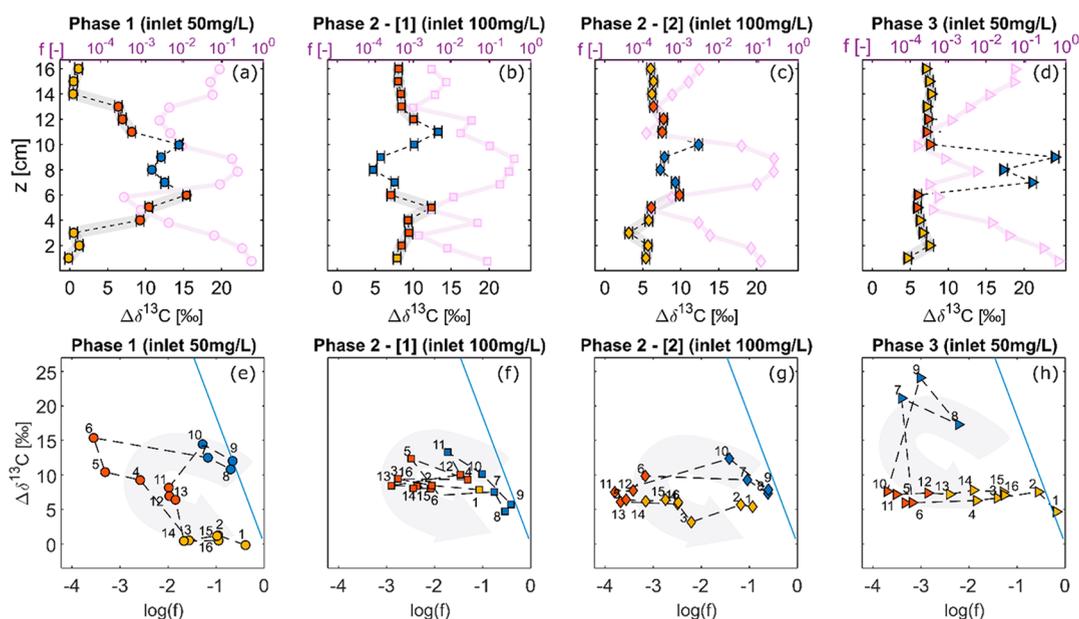
4055

Figure 4. Observable isotope fractionation in the three experimental phases with BAM inlet concentrations of 50, 100, and 50 mg/L through the central inlet port. Panels (a)−(d): vertical profiles of carbon isotope values $\Delta\delta^{13}C$ (data with error bars) and mean values of the fraction f of residual BAM concentration ($f = c_{BAM}^{biotic}/c_{BAM}^{abiotic}$, purple data points); panels (e)−(h): carbon isotope values $\Delta\delta^{13}C$ vs the fraction f—a typical representation of data under the assumption of the Rayleigh relation (eq 1). For comparison, blue solid lines represent the predicted Rayleigh relation between f and isotope values in the absence of mass-transfer limitation. Data points were labeled with the vertical outlet sampling position z = 1−16 cm. Isotope data points with gray shadow in the upper panels (a)−(d) represent the isotope values strongly constrained by mass-transfer limitation (red points) or by both mass-transfer limitation and slowdown of enzyme reaction rate (yellow data points). Blue data points represent isotope fractionation close to the Rayleigh relation. Dashed lines connect data points from adjacent ports as a guide. Error bars represent ±0.5 ‰ uncertainty of carbon isotope measurements.

Further, a widening of the BAM plume, higher remaining BAM concentrations and higher concentrations of 2,6-DCBA (i.e., incompletely catabolized substrate) were observed at the plume center when 100 mg/L of BAM were fed through the central inlet port. This observation is most likely due to a depletion of oxygen over a larger width of the plume center. Consequently, the plume fringes, where bacteria were particularly enriched, widened (Figure 3b), from the locations at z = 7 cm and z = 11 cm to the location at z = 6 cm and z = 11 cm. In addition, the degradation activity became spatially more symmetric, as seen in the profiles of f-values and metabolite-to-parent compound ratios (Figure 2e,f, third row). This observation indicates that a more symmetric distribution of biomass in the system had developed with the spread of the contaminant plume.

In phase 3 (the final phase), we decreased the inlet BAM concentration from 100 mg/L back down to 50 mg/L (day 136). After the switch the BAM concentration in the outlet ports decreased drastically after 20 h and kept decreasing in the next 4 days (from 7 mg/L to 1 mg/L at port 8). From day 140 on, changes of concentrations were relatively small, thus we considered the sampling period from day 140 to day 169 to be at quasi-steady state. An average BAM degradation efficiency of up to 99 ± 2% was reached during this quasi-steady-state sampling period (day 140 to day 169), where the deficit in the mass balance (SI Table S2) was primarily attributable to the plume center and the fringes rather than the low concentration regions (SI Figure S4). The calculated carbon assimilation rate was 7 ± 1%. The remaining BAM concentrations were generally smaller (Figure 2b), and the vertical distribution of the activity in the tank was more symmetric than in phase 1, even though the inlet concentration was the same (Figure 2e,

fourth row). In addition, the f-values at the outlet ports at z = 9−12 cm in phase 3 were about 2 orders of magnitude lower, and the isotope fractionation was generally 5−7‰ higher than the values in phase 1 (Figure 4). This line of evidence (BAM concentration, f- values, and isotope value profiles) suggests that the combined effect of the inadvertent flow fluctuation and the injection of increased substrate concentrations (priming) yielded an increased degradation capacity/activity of attached cells and led to a higher degradation of BAM compared to phase 1, despite identical BAM inlet concentrations. It also suggests that once a new quasi-steady state related to substrate concentration and flow velocity[28] had been reached, a decrease in inlet concentrations between phase 2 and phase 3 did not drive an immediate decrease in bacterial activity. Instead, it persisted for a considerable time (weeks to months).[14,33,62] Specifically, the zones of the highest attached cell numbers in phase 3 (z = 6, 9, and 10 cm, Figure 2a, fourth row) were wider than the zone covered by the ports of the highest washed-out cell numbers in the initial operational phase 1 (z = 7 and 10 cm at 50 mg/L BAM inlet concentration, Figure 2a, first row). This observation implies the persistence of biomass, established during the high-concentration phase 2, even after the BAM inlet concentration had decreased. Hence, although the plume width narrowed when the BAM inlet concentration was reduced from phase 2 to phase 3, the observed elevated degradation activity in phase 3 indicated that the attached biomass distribution and activity likely remained similar as in phase 2 at elevated BAM inlet concentration. This result contrasts with the observation in phase 1 (large washed-out cell number with overall low degradation capacity) and the widely observed loss (more than 90%) of initially adhered *Aminobacter* sp. MSH1 bacteria (e.g.,
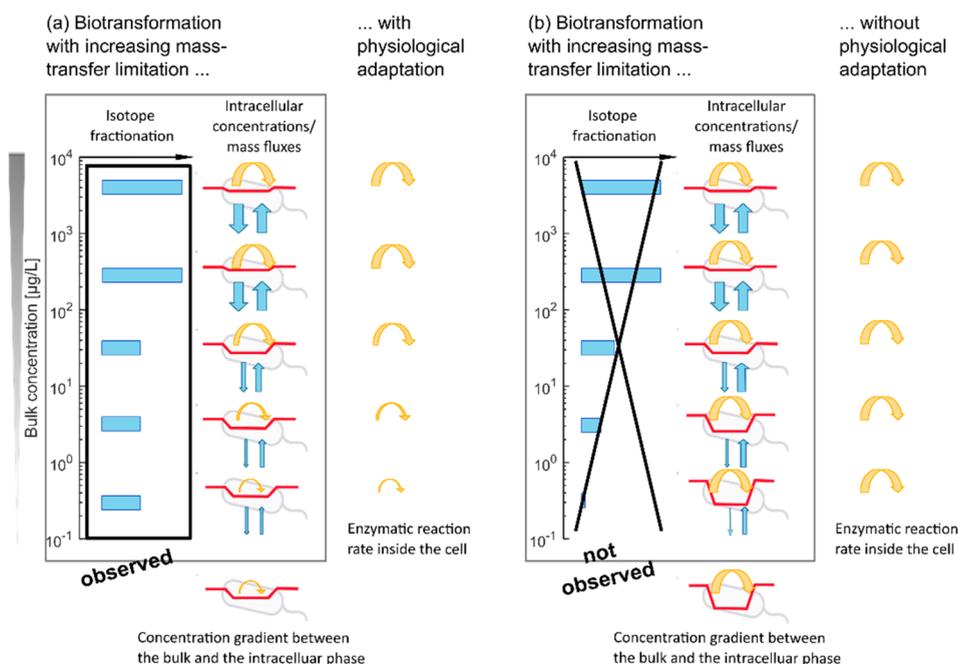
Figure 5. Isotope fractionation, mass transfer through bacterial cell membrane, and intracellular enzymatic reaction rate with decreasing substrate bulk concentration, with scenario (a) biotransformation with mass-transfer limitation and with physiological adaptation (observed in this study), and scenario (b) biotransformation with mass-transfer limitation and without physiological adaptation (not observed).

due to processes of shearing, starvation, and cell death), or of decreased BAM degradation efficiency within the first weeks after inoculation in many sand-filter experiments without priming.[15,64]

Underlying Limitations for Biodegradation over the Three Experimental Phases. To further elucidate the dynamics of the microbial population in response to concentration changes, we analyzed the isotope fractionation profile along the outlet cross-section (Figure 4).

The isotope fractionation profiles along the outlet cross-section showed a general trend similar to the one observed and accurately simulated by Sun et al.[46] At high BAM concentrations (from the center of the plume to the plume fringes, blue data points in Figure 4a−c,e−g), isotope fractionation increased with decreasing remaining BAM concentrations and decreasing f-values. These trends follow a Rayleigh behavior according to eq 2 and indicate that degradation was only limited by the availability of the electron acceptor (i.e., DO). At the plume fringes, where electron donor and acceptor mixed most efficiently, isotope values were highest, corresponding to a small f-value and a high concentration ratio of 2,6-DCBA to BAM (Figure 2e,f). At lower BAM concentrations (from the plume fringes toward the upper and lower boundaries of the tank, red data points in Figure 4), the smaller extent of isotope fractionation (compared to the isotope fractionation that the Rayleigh equation would predict with the given f-values) revealed that mass transfer became limiting ("threshold region"). Due to the slower mass-transfer rate compared to fast enzymatic turnover, many molecules with both heavy and light isotopes were transformed before they could diffuse out of the cell again, strongly masking the observable isotope fractionation in the bulk solution.

For locations where BAM concentrations were even lower (0.1−3 μg/L, in the uppermost and lowermost regions, yellow data points in Figure 4), Figure 5 illustrates two possible

scenarios. A scenario with no physiological adaptation and high enzyme activity would yield a further decrease in isotope fractionation; therefore, isotope fractionation becomes completely masked (Figure 5b). In contrast, in a scenario where physiological adaptation acted to downregulate enzyme activity to match the lower substrate availability, isotope fractionation would remain somewhat masked, but would not disappear altogether (Figure 5a). The regions with yellow data points in Figure 4 show that changes in isotope values remained consistent with the isotope values in the threshold region corresponding to the scenario in Figure 5a. This observation indicates that in this low concentration range, mass-transfer limitation further induced physiological limitation (i.e., enzyme regulation). In fact, the consistently observed small isotope fractionation over almost the whole concentration range (red and yellow data points in Figure 4d) indicates that the same extent of mass-transfer limitation prevailed throughout the gradient (with the exception of the center, where DO was limiting).

To explore this general trend of isotope fractionation in the context of an expected Rayleigh behavior (Figure 1c, eq 2), the design of our experiment in three phases enabled us to follow the relationship between isotope fractionation and the f-value over time (Figure 4e−h) and to explore whether it can confirm these conclusions about the limitations of BAM degradation at low concentrations (e.g., mass-transfer limitation, or limitation by physiological adaptation) in response to the perturbations imposed.

In phase 1, we did not observe any isotope fractionation at the upper and lower boundaries of the tank (yellow dots in Figure 4a,e, at $z = 1, 2, 3, 14, 15, 16$ cm). A potential explanation is that bacteria were in an adaptation stage after inoculation, and neither the cell population nor the degradation activity was well established throughout the tank. Therefore, in the first sampling days, the associated turnover was limited, despite favorable thermodynamic

conditions. Since we collected integrated samples over a longer time period, the original isotope ratio of nondegraded samples (BAM molecules having experienced no biodegradation) at the beginning of the sampling period may have diluted the isotope fractionation induced by biodegradation at the later stage of the sampling period. Thus, isotope fractionation may not have been discernible in the final time-integrated samples. This is consistent with our conclusion that the bottleneck of biodegradation in this experimental phase was the adaptation and establishment of the strain *Aminobacter* sp. MSH1 throughout the tank. Furthermore, even though the f-values in the upper region are approximately 2 orders of magnitude higher than the ones in the lower region, the difference of the observed isotope fractionation in the upper and lower regions is only 1−2 per mil (Figure 4a,e). As discussed in more detail below, this again is likely due to the effect of masking where similar changes in isotope values are observed irrespective of f-values.

In the first sampling period of phase 2, when the BAM inlet concentration in the central port had just been increased to 100 mg/L, the degradation hot spots where the isotope fractionation was highest were at ports $z = 5$ and 11 cm. In contrast, during the second sampling period, when the bacteria had already adapted to the change of the higher inlet concentration, the biodegradation efficiency had increased, and the plume became narrower, as indicated by the smaller f-values and higher isotope fractionation at the hot spots at $z = 6$ and 10 cm. The corresponding experimental data of this phase has recently been analyzed in detail via a numerical reactive transport model.[46] The current study builds on this work, but goes further and enables us to explore bacterial adaptation beyond this snapshot in time by following the change of biodegradation activity in the tank system over an extended time period.

In phase 3, after the BAM concentration in the central inlet port had been decreased to 50 mg/L, isotope values in the plume center (blue data points, Figure 4h) deviated from the theoretical trend of the Rayleigh relation (blue solid line, Figure 4h) and the constant isotope values in the low concentrations throughout the upper and lower regions of the tank (red and yellow data points, Figure 4h) revealed that biodegradation was limited by mass transfer throughout the tank, even in the plume center, which is an effect of the large biomass buildup during phase 2. The observation follows the trend observed during the second sampling period of phase 2 where the f-values at ports $z = 1−5$ cm and $z = 11−16$ cm increased toward the upper and lower boundaries, indicating a decreased biodegradation rate and a potential physiological limitation by adaptation (see also Sun et al.[46]). Hence, with sufficient biomass, the biodegradation efficiency of the system increased to the degree that it became limited by diffusion into the cells. Under these conditions, the changes in isotope values remained equally small at the upper and lower plume regions, whereas f-values increased with decreasing concentration, indicating a smaller extent of degradation (yellow dots). This zone of reduced degradation at $z = 1−4$, 13−16 cm was closer to the plume center compared to phases 1 and 2, which indicates a wider spread of a physiological adaptation (less active metabolism) in response to the mass-transfer limitation of substrate supply. In line with this observation, Figure 3d shows a much lower specific BAM degradation rate per cell at the upper and lower boundaries of the tank.

Thus, although the overall biodegradation efficiency was enhanced, the degradation activity was limited by a physiological adaptation of the microorganisms to the low substrate concentration. Specifically, the degradation performance in phase 3 represented a stimulated system that was more efficient compared to the initial phase 1 (50 mg/L BAM-injection). The higher biomass density at the onset of phase 3 (a legacy of the 100 mg/L injection during phase 2) drove the concentration drop in the breakthrough profiles. We hypothesize that this subsequently caused the bacteria to adapt to the low concentrations via a reduction in the cell-specific degradation activity, as indicated by the small, but consistently nonzero isotope fractionation, depicted in the scenario of Figure 5a. We reason that a higher internal activity may be difficult to sustain at low substrate turnover because of the increasing mass-transfer limitation. Such physiological adaptation (e.g., downregulation of functional genes, or reduced activity of catabolic enzymes) would result in lower bacterial activity which would prevent complete degradation of BAM. This physiological limitation of *Aminobacter* sp. MSH1, which yields reduced BAM degrading ability at low BAM concentration, has also been observed by Sekhar et al.,[23] who explained it by reduced production of the amidase BbdA that converts BAM to 2,6-DCBA due to physiological adaptation.

■ IMPLICATIONS FOR IMPROVEMENT OF BIODEGRADATION SCHEMES AND INTERPRETATION OF ISOTOPE-FRACTIONATION

Figure 5 illustrates the opportunity brought forth by this study. That is, recognizing the limitations of biodegradation while following the adaptation of a bioremediation system over time, and while exploring its adaptation to low concentrations. Initially, in a freshly inoculated sediment tank we observed a priming effect on biodegradation when we introduced intermediate disturbances in environmental conditions (such as a temporary increase of the substrate concentration and a temporary, transient flow condition) in our flow-through sediment system. The elevated degradation efficiency continued over weeks after returning to a lower inlet concentration, suggesting that such priming has the potential to establish a sustainable high degradation efficiency over a relatively long time (weeks or months). Exposing bacteria to elevated concentrations of the target compound and changing the flow regime, is, therefore, a potential strategy to improve the degradation of organic contaminants in water treatment plants or in situ remediation. Our findings are in line with the ecological concept of the 'intermediate disturbance hypothesis':[65,66] that functional microbial populations are stimulated when there are regular disturbances that are neither too rare nor too frequent, and neither too intensive nor too moderate.

Moreover, our results suggest that such periodic intermediate stimulation may be urgently needed. Our observations indicate that biodegradation activity became not only limited by mass-transfer limitations, but also by bacterial adaptation to low concentrations over time. Specifically, while our isotope data are consistent with the conclusions of our recent work,[46] that mass transfer becomes *partially* rate-limiting at low concentrations (Figure 4a−c), the long-term results of the present study suggest that this is only part of the picture. Figure 4d shows that mass transfer never became *completely* rate-limiting meaning that a scenario as depicted in Figure 5b was not observed. Rather Figure 4d implies a scenario as depicted in Figure 5a: The more the system was stimulated

and adapted over time, the more uniform was the extent of isotope fractionation throughout the gradient, irrespective of concentrations. (Note: An exception is the plume center where oxygen was partly limiting.) The fact that we observed some isotope fractionation even at low concentrations, implies that even there, molecules with heavy isotopes were discriminated by the slow enzymatic reactions and had the opportunity to diffuse back to the bulk solution to be observed by measurements (Figure 5a). Thus, as illustrated in the conceptual diagram of Figure 5a, bacteria seemed to adapt their enzyme activity to the prevailing concentrations thereby tending to operate "at the brink of substrate supply". The *uniform* extent of isotope fractionation, irrespective of f (Figure 4d), suggests that, in response to mass-transfer limitations, physiological limitation (i.e., a reduced enzymatic reaction rate) to prevailing concentrations took place (Figure 5a), which inevitably limited the biodegradation performance throughout the spatial concentration gradient. This interplay is modeled in SI Figure S6, which illustrates the influence of bulk concentration and maximum enzymatic reaction rate on the observable isotope fractionation with the consideration of the mass-transfer process through the bacterial cell membrane.

To make use of this insight for water treatment technologies, approaches may build on a hybrid concept brought forward by Hylling et al.[67] Here, membrane filtration by a reverse osmosis (RO) unit is combined with biodegradation in a sand filter system that is continuously fed with RO retentate. If a particularly concentrated retentate solution is used to periodically regenerate the sand filter system through backwashing, this could potentially provide for such a regular disturbance/priming and further stimulate the bacterial degradation capacity in the inoculated sand filter system such that it would show activity beyond regulation "at the brink of substrate supply". In fact, our results are in line with recent work by Ellegaard-Jensen et al.,[68] who observed excellent biodegradation performance in their inoculated sand filter for up to 60 days, and a decline in the BAM removal rate to 60% after 150 days,[68] suggesting that also therein restimulation may have been needed.

Future investigations should therefore focus on pilot sand-filter experiments that introduce such intermediate disturbances/priming during the backwashing stage, or that focus on the influence of multiple carbon sources on such a priming effect. For a conceptual assessment of in situ biodegradation at contaminated sites, priming effects or intermediate system disturbances should be considered as a potential trigger that enriches biomass and optimizes the spread of the bacteria. To reach a more generalizable conclusion, investigations in more complex (natural) environmental systems, with multiple carbon sources, a higher complexity of the microbial community, and a wider range of organic pollutants are still needed. In such endeavors the approach delineated here—combined analysis of isotope fractionation and residual substrate fraction—can greatly help reveal mass-transfer and physiological limitations and, therefore, aid in "tuning" in situ bioremediation for complete elimination of organic micro-pollutants.

ASSOCIATED CONTENT

ⓢ Supporting Information

The Supporting Information is available free of charge at https://pubs.acs.org/doi/10.1021/acs.est.1c05259.

Additional details for the Experimental Section (PDF)

AUTHOR INFORMATION

Corresponding Author

Martin Elsner − *Institute of Groundwater Ecology, Helmholtz Zentrum München, 85764 Neuherberg, Germany; Chair of Analytical Chemistry and Water Chemistry, Technical University of Munich, 85748 Garching, Germany;* ⓞ orcid.org/0000-0003-4746-9052; Phone: +49 89 2180-78232; Email: m.elsner@tum.de

Authors

Fengchao Sun − *Institute of Groundwater Ecology, Helmholtz Zentrum München, 85764 Neuherberg, Germany; Chair of Analytical Chemistry and Water Chemistry, Technical University of Munich, 85748 Garching, Germany*

Adrian Mellage − *Center for Applied Geoscience, University of Tübingen, 72076 Tübingen, Germany;* ⓞ orcid.org/0000-0003-2708-4518

Zhe Wang − *Institute of Groundwater Ecology, Helmholtz Zentrum München, 85764 Neuherberg, Germany; Chair of Ecological Microbiology, University of Bayreuth, 95448 Bayreuth, Germany; School of Life Sciences, Technical University of Munich, 85354 Freising, Germany*

Rani Bakkour − *Chair of Analytical Chemistry and Water Chemistry, Technical University of Munich, 85748 Garching, Germany*

Christian Griebler − *Department of Functional and Evolutionary Ecology, University of Vienna, 1030 Vienna, Austria*

Martin Thullner − *Department of Environmental Microbiology, UFZ—Helmholtz Centre for Environmental Research, 30418 Leipzig, Germany;* ⓞ orcid.org/0000-0001-9723-4601

Olaf A. Cirpka − *Center for Applied Geoscience, University of Tübingen, 72076 Tübingen, Germany;* ⓞ orcid.org/0000-0003-3509-4118

Complete contact information is available at:
https://pubs.acs.org/10.1021/acs.est.1c05259

Author Contributions

The manuscript was written through contributions of all authors. All authors have given approval to the final version of the manuscript.

Notes

The authors declare no competing financial interest.

ACKNOWLEDGMENTS

REFERENCES

(1) Schwarzenbach, R. P.; Escher, B. I.; Fenner, K.; Hofstetter, T. B.; Johnson, C. A.; Von Gunten, U.; Wehrli, B. The challenge of

micropollutants in aquatic systems. *Science* **2006**, *313* (5790), 1072−1077.

(2) Tang, F. H.; Lenzen, M.; McBratney, A.; Maggi, F. Risk of pesticide pollution at the global scale. *Nat. Geosci.* **2021**, *14* (4), 206−210.

(3) Bedient, P. B.; Rifai, H. S.; Newell, C. J. *Groundwater Contamination: Transport and Remediation*; Prentice-Hall International, Inc., 1994.

(4) EU, E. C. *Drinking Water Directive (COUNCIL DIRECTIVE 98/83/EC)*; Official Journal of the European Communities, 1998.

(5) Ellegaard-Jensen, L.; Horemans, B.; Raes, B.; Aamand, J.; Hansen, L. H. Groundwater contamination with 2,6-dichlorobenzamide (BAM) and perspectives for its microbial removal. *Appl. Environ. Microbiol.* **2017**, *101* (13), 5235−5245.

(6) Vandermaesen, J.; Horemans, B.; Degryse, J.; Boonen, J.; Walravens, E.; Springael, D. Mineralization of the Common Groundwater Pollutant 2,6-Dichlorobenzamide (BAM) and its Metabolite 2,6-Dichlorobenzoic Acid (2,6-DCBA) in Sand Filter Units of Drinking Water Treatment Plants. *Environ. Sci. Technol.* **2016**, *50* (18), 10114−22.

(7) Pukkila, V.; Kontro, M. H. Dichlobenil and 2,6-dichlorobenzamide (BAM) dissipation in topsoil and deposits from groundwater environment within the boreal region in southern Finland. *Environ. Sci. Pollut. Res.* **2014**, *21* (3), 2289−2297.

(8) Sorensen, S. R.; Holtze, M. S.; Simonsen, A.; Aamand, J. Degradation and mineralization of nanomolar concentrations of the herbicide dichlobenil and its persistent metabolite 2,6-dichlorobenzamide by Aminobacter spp. isolated from dichlobenil-treated soils. *Appl. Environ. Microbiol.* **2007**, *73* (2), 399−406.

(9) National Center for Biotechnology Information. PubChem Annotation Record for 2,6-Dichlorobenzamide, Source: Hazardous Substances Data Bank (HSDB) PubChem, https://pubchem.ncbi.nlm.nih.gov/source/hsdb/2728 (accessed 2021/6/18).

(10) Van Leeuwen, C. J.; Maas, H. The aquatic toxicity of 2,6-dichlorobenzamide (BAM), a degradation product of the herbicide dichlobenil. *Environ. Pollut, Ser. A* **1985**, *37* (2), 105−115.

(11) Clausen, L.; Larsen, F.; Albrechtsen, H.-J. Sorption of the herbicide dichlobenil and the metabolite 2, 6-dichlorobenzamide on soils and aquifer sediments. *Environ. Sci. Technol.* **2004**, *38* (17), 4510−4518.

(12) Zhang, S.; Mao, G.; Crittenden, J.; Liu, X.; Du, H. Groundwater remediation from the past to the future: A bibliometric analysis. *Water Res.* **2017**, *119*, 114−125.

(13) Cycoń, M.; Mrozik, A.; Piotrowska-Seget, Z. Bioaugmentation as a strategy for the remediation of pesticide-polluted soil: A review. *Chemosphere* **2017**, *172*, 52−71.

(14) Meckenstock, R. U.; Elsner, M.; Griebler, C.; Lueders, T.; Stumpp, C.; Aamand, J.; Agathos, S. N.; Albrechtsen, H. J.; Bastiaens, L.; Bjerg, P. L.; Boon, N.; Dejonghe, W.; Huang, W. E.; Schmidt, S. I.; Smolders, E.; Sorensen, S. R.; Springael, D.; van Breukelen, B. M. Biodegradation: Updating the concepts of control for microbial cleanup in contaminated aquifers. *Environ. Sci. Technol.* **2015**, *49* (12), 7073−81.

(15) Albers, C. N.; Feld, L.; Ellegaard-Jensen, L.; Aamand, J. Degradation of trace concentrations of the persistent groundwater pollutant 2,6-dichlorobenzamide (BAM) in bioaugmented rapid sand filters. *Water Res.* **2015**, *83*, 61−70.

(16) Ellegaard-Jensen, L.; Albers, C. N.; Aamand, J. Protozoa graze on the 2, 6-dichlorobenzamide (BAM)-degrading bacterium Aminobacter sp. MSH1 introduced into waterworks sand filters. *Appl. Microbiol. Biotechnol.* **2016**, *100* (20), 8965−8973.

(17) Schultz-Jensen, N.; Knudsen, B. E.; Frkova, Z.; Aamand, J.; Johansen, T.; Thykaer, J.; Sorensen, S. R. Large-scale bioreactor production of the herbicide-degrading Aminobacter sp. strain MSH1. *Appl. Microbiol. Biotechnol.* **2014**, *98* (5), 2335−44.

(18) Horemans, B.; Raes, B.; Vandermaesen, J.; Simanjuntak, Y.; Brocatus, H.; T'Syen, J.; Degryse, J.; Boonen, J.; Wittebol, J.; Lapanje, A.; Sorensen, S. R.; Springael, D. Biocarriers Improve Bioaugmentation Efficiency of a Rapid Sand Filter for the Treatment of 2,6-Dichlorobenzamide-Contaminated Drinking Water. *Environ. Sci. Technol.* **2017**, *51* (3), 1616−1625.

(19) Kjaergaard Nielsen, T.; Horemans, B.; Lood, C.; T'Syen, J.; van Noort, V.; Lavigne, R.; Ellegaard-Jensen, L.; Hylling, O.; Aamand, J.; Springael, D., Analyses of the complete genome sequence of 2, 6-dichlorobenzamide (BAM) degrader Aminobacter sp. MSH1 suggests a polyploid chromosome, phylogenetic reassignment, and functions of (un) stable plasmids. *bioRxiv* **2021**.

(20) Raes, B.; Horemans, B.; Rentsch, D.; T'Syen, J.; Ghequire, M. G. K.; De Mot, R.; Wattiez, R.; Kohler, H.-P. E.; Springael, D. Aminobacter sp. MSH1 mineralizes the groundwater micropollutant 2,6-dichlorobenzamide through a unique chlorobenzoate catabolic pathway. *Environ. Sci. Technol.* **2019**, *53* (17), 10146−10156.

(21) T'Syen, J.; Tassoni, R.; Hansen, L.; Sorensen, S. J.; Leroy, B.; Sekhar, A.; Wattiez, R.; De Mot, R.; Springael, D. Identification of the Amidase BbdA That Initiates Biodegradation of the Groundwater Micropollutant 2,6-dichlorobenzamide (BAM) in Aminobacter sp. MSH1. *Environ. Sci. Technol.* **2015**, *49* (19), 11703−13.

(22) Sjoholm, O. R.; Nybroe, O.; Aamand, J.; Sorensen, J. 2,6-Dichlorobenzamide (BAM) herbicide mineralisation by Aminobacter sp. MSH1 during starvation depends on a subpopulation of intact cells maintaining vital membrane functions. *Environ. Pollut.* **2010**, *158* (12), 3618−25.

(23) Sekhar, A.; Horemans, B.; Aamand, J.; Sorensen, S. R.; Vanhaecke, L.; Bussche, J. V.; Hofkens, J.; Springael, D. Surface Colonization and Activity of the 2,6-Dichlorobenzamide (BAM) Degrading Aminobacter sp. Strain MSH1 at Macro- and Micropollutant BAM Concentrations. *Environ. Sci. Technol.* **2016**, *50* (18), 10123−33.

(24) Thullner, M.; Kampara, M.; Richnow, H. H.; Harms, H.; Wick, L. Y. Impact of bioavailability restrictions on microbially induced stable isotope fractionation. 1. Theoretical calculation. *Environ. Sci. Technol.* **2008**, *42* (17), 6544−6551.

(25) Bosma, T. N. P.; Middeldorp, P. J. M.; Schraa, G.; Zehnder, A. J. B. Mass Transfer Limitation of Biotransformation: Quantifying Bioavailability. *Environ. Sci. Technol.* **1997**, *31* (1), 248−252.

(26) Kundu, K.; Marozava, S.; Ehrl, B.; Merl-Pham, J.; Griebler, C.; Elsner, M. Defining lower limits of biodegradation: atrazine degradation regulated by mass transfer and maintenance demand in Arthrobacter aurescens TC1. *ISME J.* **2019**, *13* (9), 2236−2251.

(27) Eckert, D.; Kürzinger, P.; Bauer, R.; Griebler, C.; Cirpka, O. A. Fringe-controlled biodegradation under dynamic conditions: Quasi 2-D flow-through experiments and reactive-transport modeling. *J. Contam. Hydrol.* **2015**, *172*, 100−111.

(28) Grosbacher, M.; Eckert, D.; Cirpka, O. A.; Griebler, C. Contaminant concentration versus flow velocity: drivers of biodegradation and microbial growth in groundwater model systems. *Biodegradation* **2018**, *29* (3), 211−232.

(29) Prommer, H.; Barry, D. A.; Davis, G. B. Modelling of physical and reactive processes during biodegradation of a hydrocarbon plume under transient groundwater flow conditions. *J. Contam. Hydrol.* **2002**, *59* (1), 113−131.

(30) Cirpka, O. A.; Attinger, S., Effective dispersion in heterogeneous media under random transient flow conditions. *Water Resour. Res.* **2003**, *39* (9). DOI: 10.1029/2002WR001931

(31) Rodríguez-Escales, P.; Fernàndez-Garcia, D.; Drechsel, J.; Folch, A.; Sanchez-Vila, X. Improving degradation of emerging organic compounds by applying chaotic advection in Managed Aquifer Recharge in randomly heterogeneous porous media. *Water Resour. Res.* **2017**, *53* (5), 4376−4392.

(32) Andrews, J. H.; Harris, R. F. r- and K-Selection and Microbial Ecology. In *Advances in Microbial Ecology*; Marshall, K. C., Ed.; Springer US: Boston, MA, 1986; pp 99−147.

(33) Mellage, A.; Eckert, D.; Grosbacher, M.; Inan, A. Z.; Cirpka, O. A.; Griebler, C. Dynamics of suspended and attached aerobic toluene degraders in small-scale flow-through sediment systems under growth and starvation conditions. *Environ. Sci. Technol.* **2015**, *49* (12), 7161−9.

(34) Torstensson, L. Microbial decomposition of herbicides in the soil. *Outlook Agric* **1988**, *17* (3), 120−124.

(35) Greenwood, P. F.; Wibrow, S.; George, S. J.; Tibbett, M. Hydrocarbon biodegradation and soil microbial community response to repeated oil exposure. *Org. Geochem.* **2009**, *40* (3), 293−300.

(36) Kundu, K.; Weber, N.; Griebler, C.; Elsner, M. Phenotypic heterogeneity as key factor for growth and survival under oligotrophic conditions. *Environ. Microbiol.* **2020**, *22* (8), 3339−3356.

(37) Sun, F.; Peters, J.; Thullner, M.; Cirpka, O. A.; Elsner, M. Magnitude of diffusion- and transverse dispersion-induced isotope fractionation of organic compounds in aqueous systems. *Environ. Sci. Technol.* **2021**, *55* (8), 4772−4782.

(38) Wanner, P.; Hunkeler, D. Isotope fractionation due to aqueous phase diffusion - What do diffusion models and experiments tell? - A review. *Chemosphere* **2019**, *219*, 1032−1043.

(39) Kuntze, K.; Eisenmann, H.; Richnow, H.-H.; Fischer, A. Compound-Specific Stable Isotope Analysis (CSIA) for Evaluating Degradation of Organic Pollutants: An Overview of Field Case Studies. *Anaerobic Utilization of Hydrocarbons, Oils, and Lipids* **2020**, 323−360.

(40) Reinnicke, S.; Simonsen, A.; Sorensen, S. R.; Aamand, J.; Elsner, M. C and N isotope fractionation during biodegradation of the pesticide metabolite 2,6-dichlorobenzamide (BAM): potential for environmental assessments. *Environ. Sci. Technol.* **2012**, *46* (3), 1447−54.

(41) Mariotti, A.; Germon, J. C.; Hubert, P.; Kaiser, P.; Letolle, R.; Tardieux, A.; Tardieux, P. Experimental determination of nitrogen kinetic isotope fractionation: Some principles; illustration for the denitrification and nitrification processes. *Plant Soil* **1981**, *62* (3), 413−430.

(42) Breukelen, B. M. V.; Prommer, H. Beyond the Rayleigh Equation: Reactive Transport Modeling of Isotope Fractionation Effects to Improve Quantification of Biodegradation. *Environ. Sci. Technol.* **2008**, *42* (7), 2457−2463.

(43) Rayleigh, L. Theoretical considerations respecting the separation of gases by diffusion and similar processes. *London, Edinburgh Dublin Philos. Mag. J. Sci.* **1896**, *42* (259), 493−498.

(44) Hoefs, J. *Stable Isotope Geochemistry*, 9th ed.; Springer: Cham, 2021; pp XXV, 504.

(45) Ehrl, B. N.; Kundu, K.; Gharasoo, M.; Marozava, S.; Elsner, M. Rate-Limiting Mass Transfer in Micropollutant Degradation Revealed by Isotope Fractionation in Chemostat. *Environ. Sci. Technol.* **2019**, *53* (3), 1197−1205.

(46) Sun, F.; Mellage, A.; Gharasoo, M.; Melsbach, A.; Cao, X.; Zimmermann, R.; Griebler, C.; Thullner, M.; Cirpka, O. A.; Elsner, M. Mass-transfer-limited biodegradation at low concentrations—evidence from reactive transport modeling of isotope profiles in a bench-scale aquifer. *Environ. Sci. Technol.* **2021**, *55* (11), 7386−7397.

(47) Kampara, M.; Thullner, M.; Richnow, H. H.; Harms, H.; Wick, L. Y. Impact of bioavailability restrictions on microbially induced stable isotope fractionation. 2. Experimental evidence. *Environ. Sci. Technol.* **2008**, *42* (17), 6552−6558.

(48) Kampara, M.; Thullner, M.; Harms, H.; Wick, L. Y. Impact of cell density on microbially induced stable isotope fractionation. *Appl. Microbiol. Biotechnol.* **2009**, *81* (5), 977−985.

(49) Bauer, R. D.; Maloszewski, P.; Zhang, Y.; Meckenstock, R. U.; Griebler, C. Mixing-controlled biodegradation in a toluene plume–results from two-dimensional laboratory experiments. *J. Contam. Hydrol.* **2008**, *96* (1−4), 150−68.

(50) Muniruzzaman, M.; Rolle, M. Experimental investigation of the impact of compound-specific dispersion and electrostatic interactions on transient transport and solute breakthrough. *Water Resour. Res.* **2017**, *53* (2), 1189−1209.

(51) Sun, F.; Peters, J.; Thullner, M.; Cirpka, O. A.; Elsner, M., Magnitude of diffusion- and transverse dispersion-induced isotope fractionation of organic compounds in aqueous systems. *Environ. Sci. Technol.* **2021**, *55*4772−4782

(52) Jensen, G. G.; Bjorklund, E.; Simonsen, A.; Halling-Sorensen, B. Determination of 2,6-dichlorobenzamide and its degradation products in water samples using solid-phase extraction followed by liquid chromatography-tandem mass spectrometry. *J. Chromatogr A* **2009**, *1216* (27), 5199−206.

(53) Bayer, A.; Drexel, R.; Weber, N.; Griebler, C. Quantification of aquatic sediment prokaryotes—A multiple-steps optimization testing sands from pristine and contaminated aquifers. *Limnologica* **2016**, *56*, 6−13.

(54) Pilloni, G.; von Netzer, F.; Engel, M.; Lueders, T. Electron acceptor-dependent identification of key anaerobic toluene degraders at a tar-oil-contaminated aquifer by Pyro-SIP. *FEMS Microbiol. Ecol.* **2011**, *78* (1), 165−75.

(55) Horemans, B.; Vandermaesen, J.; Sekhar, A.; Rombouts, C.; Hofkens, J.; Vanhaecke, L.; Springael, D., Aminobacter sp. MSH1 invades sand filter community biofilms while retaining 2,6-dichlorobenzamide degradation functionality under C- and N-limiting conditions. *FEMS Microbiol. Ecol.* **2017**, *93* (6). DOI: 10.1093/femsec/fix064

(56) Bengtsson, G. Growth and metabolic flexibility in groundwater bacteria. *Microb. Ecol.* **1989**, *18* (3), 235−248.

(57) Griebler, C.; Mindl, B.; Slezak, D.; Geiger-Kaiser, M. Distribution patterns of attached and suspended bacteria in pristine and contaminated shallow aquifers studied with an in situ sediment exposure microcosm. *Aquat. Microb. Ecol.* **2002**, *28* (2), 117−129.

(58) Griebler, C.; Mindl, B.; Slezak, D. Combining DAPI and SYBR Green II for the enumeration of total bacterial numbers in aquatic sediments. *Int. Rev. Hydrobiol.* **2001**, *86* (4−5), 453−465.

(59) Harvey, R. W.; Smith, R. L.; George, L. Effect of organic contamination upon microbial distributions and heterotrophic uptake in a Cape Cod, Mass., aquifer. *Appl. Environ. Microbiol.* **1984**, *48* (6), 1197−202.

(60) Harvey, R. W.; George, L. H. Growth determinations for unattached bacteria in a contaminated aquifer. *Appl. Environ. Microbiol.* **1987**, *53* (12), 2992−2996.

(61) Godsy, E. M. *Methanogenic Biodegradation of Creosote-Derived Contaminants in Natural and Simulated Ground Water Ecosystems*; Stanford University, 1993.

(62) Herzyk, A.; Fillinger, L.; Larentis, M.; Qiu, S.; Maloszewski, P.; Hunniger, M.; Schmidt, S. I.; Stumpp, C.; Marozava, S.; Knappett, P. S. K.; Elsner, M.; Meckenstock, R.; Lueders, T.; Griebler, C. Response and recovery of a pristine groundwater ecosystem impacted by toluene contamination - A meso-scale indoor aquifer experiment. *J. Contam. Hydrol.* **2017**, *207*, 17−30.

(63) Murphy, E. M.; Ginn, T. R. Modeling microbial processes in porous media. *Hydrogeol. J.* **2000**, *8* (1), 142−158.

(64) Albers, C. N.; Jacobsen, O. S.; Aamand, J. Using 2,6-dichlorobenzamide (BAM) degrading Aminobacter sp. MSH1 in flow through biofilters–initial adhesion and BAM degradation potentials. *Appl. Environ. Microbiol.* **2014**, *98* (2), 957−67.

(65) Gaedeke, A.; Sommer, U. The influence of the frequency of periodic disturbances on the maintenance of phytoplankton diversity. *Oecologia* **1986**, *71* (1), 25−28.

(66) Carrero-Colón, M.; Nakatsu, C. H.; Konopka, A. Effect of Nutrient Periodicity on Microbial Community Dynamics. *Appl. Environ. Microbiol.* **2006**, *72* (5), 3175−3183.

(67) Hylling, O.; Nikbakht Fini, M.; Ellegaard-Jensen, L.; Muff, J.; Madsen, H. T.; Aamand, J.; Hansen, L. H. A novel hybrid concept for implementation in drinking water treatment targets micropollutant removal by combining membrane filtration with biodegradation. *Sci. Total Environ.* **2019**, *694*, 133710.

(68) Ellegaard-Jensen, L.; Schostag, M. D.; Nikbakht Fini, M.; Badawi, N.; Gobbi, A.; Aamand, J.; Hansen, L. H. Bioaugmented sand filter columns provide stable removal of pesticide residue from membrane retentate. *Front. water.* **2020**, *2* (55), 603567.